Chapter II Guidance Laws, Obstacle Avoidance, Artificial Potential Functions

Distinguished Professor Anthony J. Healey
Director, Center for AUV Research
Naval Postgraduate School
Monterey, CA. 93943
(healey@nps.edu)

INTRODUCTION

In the context of autonomy for underwater vehicles, we assume that a usual suite of feedback controllers are present in the form of autopilot functions that provide for the regulation of vehicle speed, heading, and depth or altitude. In this chapter, we consider the topic of Guidance Laws, Obstacle Avoidance and the use of Artificial Potential Functions (APFs). This topic deals with the computations required to plan and develop paths and commands, which are used by these auto-pilots. Simple guidance laws such as "proportional guidance' have been used for many years in missiles to provide interception with targets. Lateral accelerations are commanded proportional to the rate of change of line of sight. So long as the chaser vehicle has a speed advantage over the non-maneuvering target, simply reducing the angle of line of sight to zero will result in an interception.

For applications with unmanned underwater vehicles, guidance laws allow vehicles to follow paths constructed in conjunction with mission objectives. For instance, in a mine-hunting mission, we often design paths that 'mow the lawn'. An objective area is defined; tracks are developed, with track spacing defined according to the swath width of the side-scanning sonar and a required overlap, so that complete coverage of the area is obtained. Increasing overlap leads to increased probability of detection at the expense of overall search rate. These tracks are defined by starting and ending

Report Documentation Page

Form Approved
OMB No. 0704-0188

1. REPORT DATE	2. REPORT TYPE	3. DATES COVERED
MAR 2006		**00-00-2006 to 00-00-2006**

4. TITLE AND SUBTITLE	5a. CONTRACT NUMBER
Chapter II Guidance Laws, Obstacle Avoidance, Artificial Potential Functions	5b. GRANT NUMBER
	5c. PROGRAM ELEMENT NUMBER
6. AUTHOR(S)	5d. PROJECT NUMBER
	5e. TASK NUMBER
	5f. WORK UNIT NUMBER
7. PERFORMING ORGANIZATION NAME(S) AND ADDRESS(ES) **Naval Postgraduate School,Center for Autonomous Underwater Vehicle Research,Monterey,CA,93943**	8. PERFORMING ORGANIZATION REPORT NUMBER
9. SPONSORING/MONITORING AGENCY NAME(S) AND ADDRESS(ES)	10. SPONSOR/MONITOR'S ACRONYM(S)
	11. SPONSOR/MONITOR'S REPORT NUMBER(S)

12. DISTRIBUTION/AVAILABILITY STATEMENT
Approved for public release; distribution unlimited

13. SUPPLEMENTARY NOTES
IEE Control Series 69, Eds. Roberts and Sutton, March, 2006

14. ABSTRACT

15. SUBJECT TERMS

16. SECURITY CLASSIFICATION OF:			17. LIMITATION OF ABSTRACT	18. NUMBER OF PAGES	19a. NAME OF RESPONSIBLE PERSON
a. REPORT **unclassified**	b. ABSTRACT **unclassified**	c. THIS PAGE **unclassified**	**Same as Report (SAR)**	**35**	

points (way-points) and the vehicle is guided along these tracks by a track following guidance law that drives the cross-track position error to zero. In this mode, the vehicle closely follows the defined path in position only, but no attempt is made to follow a specific trajectory in both time and position. Trajectory tracking (Kaminer, et. al., 1998) which may be necessary if formation control is required, implies that not only cross-track but also the corresponding along track errors are controlled. Clearly this added requirement means that some position along the track determined by some moving point on the trajectory is to be maintained. In essence trajectory following is more complex and requires speed as well as heading control. Another related topic involves the design of optimal paths to follow for example in (Milam, 2003) . In this sense, path length is minimized subject to curvature and other constraints rather than allowing the vehicle to respond to way-points, with no guaranteed coverage in tight spaces between closely positioned points. In open ocean conditions it is rare that such precision in an actual path is important, but it could be important in obstacle avoidance maneuvering where minimum distances between vehicles and obstacles should be observed.

By reference to the Figure 1 below, the auto-pilots for Speed Heading and Depth control are assumed to be already present in the vehicle dynamics. The notion of a guidance system is based around the idea that the heading command is taken from the guidance system. It allows for track following, cross track error control and for obstacle avoidance, and as such requires knowledge of vehicle position from a navigation system, and knowledge of the mission so that track plans can be made and modified. In the discussion of obstacle avoidance guidance, we include the methods of artificial potential fields, curved path deviation planning, and reactive avoidance.

The system is driven from the perceptory inputs modified by sonar signal processing, and algorithms for obstacle detection, obstacle tracking, location and mapping.

VEHICLE GUIDANCE, TRACK FOLLOWING

To follow a set of straight line tracks, forms the basis of many simple guidance requirements. In this section, a simple line of sight (LOS) guidance law is described. It is supplemented with a simple cross track error term for better performance in cross

Autonomous Underwater Vehicle Guidance System

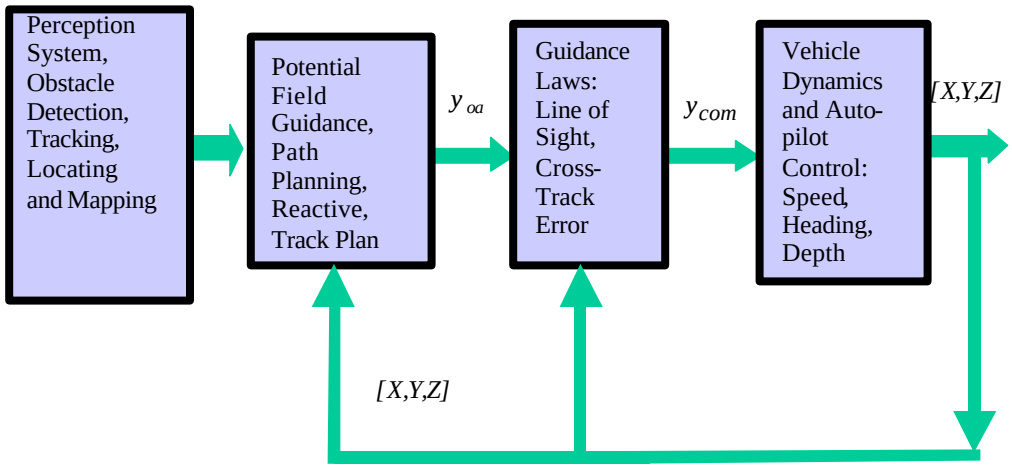

Figure 1 Overview of Vehicle Guidance Functions

currents, and a sliding mode controller is presented that has been experimentally validated under a wide variety of conditions. Other works have studied similar problems for land robots, (for example, smooth path planning in Kanayama and Hartman, 1997) and usually develop a stable guidance law based on cross track error which returns the vehicle to the desired path.

In all simulations shown later in this chapter, the same vehicle dynamics model is used, taken from the REMUS AUV as explained in earlier work (Fodrea and Healey, 2003) and the steering auto-pilot is designed according to a sliding mode methodology (Marco and Healey, 2001). The hydrodynamic coefficients are given in (Fodrea and Healey, 2003.

Vehicle Steering Model

Using the coefficients given below, and with standard nomenclature for underwater vehicles (Healey, Class Notes, 2001),

$$\begin{bmatrix} m-Y_{\dot{v}_r} & -Y_{\dot{r}} & 0 \\ -N_{\dot{v}_r} & I_{zz}-N_{\dot{r}} & 0 \\ 0 & 0 & 1 \end{bmatrix} \begin{bmatrix} \dot{v}_r \\ \dot{r} \\ \dot{y} \end{bmatrix} = \begin{bmatrix} Y_{v_r} & Y_r - mU_0 & 0 \\ N_{v_r} & N_r & 0 \\ 0 & 1 & 0 \end{bmatrix} \begin{bmatrix} v_r \\ r \\ y \end{bmatrix} + \begin{bmatrix} Y_d \\ N_d \\ 0 \end{bmatrix} d_r(t)$$

$$\begin{bmatrix} \dot{v}_r \\ \dot{r} \\ \dot{y} \end{bmatrix} = \begin{bmatrix} m-Y_{\dot{v}_r} & -Y_{\dot{r}} & 0 \\ -N_{\dot{v}_r} & I_{zz}-N_{\dot{r}} & 0 \\ 0 & 0 & 1 \end{bmatrix}^{-1} \begin{bmatrix} Y_{v_r} & Y_r - mU_0 & 0 \\ N_{v_r} & N_r & 0 \\ 0 & 1 & 0 \end{bmatrix} \begin{bmatrix} v_r \\ r \\ y \end{bmatrix} + \begin{bmatrix} m-Y_{\dot{v}_r} & -Y_{\dot{r}} & 0 \\ -N_{\dot{v}_r} & I_{zz}-N_{\dot{r}} & 0 \\ 0 & 0 & 1 \end{bmatrix}^{-1} \begin{bmatrix} Y_d \\ N_d \\ 0 \end{bmatrix} d_r(t) \quad (1)$$

Table of Data for the REMUS Model Use in Simulations

$Y_{\dot{v}_r}$	-3.55exp01 kg
$Y_{\dot{r}}$	1.93 kg m/rad
Y_{v_r}	-6.66exp01 kg/s (Same as Z_w)
Y_r	2.2 kg m/s (Same as Z_q)
$N_{\dot{v}_r}$	1.93 kg m
$N_{\dot{r}}$	-4.88 kg m^2/rad
N_{v_r}	-4.47 kg m/s
N_r	-6.87 kg m^2/s (Same as M_q)
N_d	-3.46exp01/3.5 kg m/s^2

Y_d	5.06exp01/3.5 kg m/s^2

m= 30.48 kg I_{zz}= 3.45 kg m2/rad
Table of Hydrodynamic and Inertial Parameters for REMUS Steering Dynamics
with the modifications to the values taken initially from Prestero, (2001),

and in more compact form

$$\dot{\boldsymbol{x}}(t) = \boldsymbol{A}\boldsymbol{x}(t) + \boldsymbol{b}u(t) \tag{2}$$

with the path response being taken from

$$\begin{aligned} \dot{X} &= U_0 \cos y \; - v_r \sin y \; + U_{cx} \\ \dot{Y} &= U_0 \sin y \; + v_r \cos y \; + U_{cy} \end{aligned} \tag{3}$$

and

$$\boldsymbol{A} = \begin{bmatrix} m - Y_{\dot{v}_r} & -Y_{\dot{r}} & 0 \\ -N_{\dot{v}_r} & I_{zz} - N_{\dot{r}} & 0 \\ 0 & 0 & 1 \end{bmatrix}^{-1} \begin{bmatrix} Y_{v_r} & Y_r - mU_0 & 0 \\ N_{v_r} & N_r & 0 \\ 0 & 0 & 1 \end{bmatrix}; \quad \boldsymbol{B} = \begin{bmatrix} m - Y_{\dot{v}_r} & -Y_{\dot{r}} & 0 \\ -N_{\dot{v}_r} & I_{zz} - N_{\dot{r}} & 0 \\ 0 & 0 & 1 \end{bmatrix}^{-1} \begin{bmatrix} Y_d \\ N_d \\ 0 \end{bmatrix}$$

$$\text{where } \boldsymbol{x}(t) = [v_r \quad r \quad y\;]; u(t) = d_r(t) \tag{4}$$

In the above, U_{cx} and U_{cy} are Northerly and Easterly water currents respectively. With this in mind, any steering control law may be used, but for the sake of further discussion lets use the sliding mode control,

$$\begin{aligned} d_r(t) &= K_1 v(t) + K_2 r(t) + h \tanh(s(t)/f); \\ s(t) &= s_1(y_{com(LOS(i))} - y(t)) + s_2(r_{com}(t) - r(t)) - s_3 v(t); \end{aligned} \tag{5}$$

where, for the REMUS vehicle model, the constants, based on pole placement are taken to be: s_1=0.8647 ;s_2=0.5004 ; s_3 = 0.0000; h =0.5000 ; f = 0.1000 ; K_1 = 0.0000 ;K_2 = 0.6000 ; (6)

The coefficients of the side slip velocity have been zeroed since it is not practical to include that particular sensor in the control because of noise levels, and it has been found that the stability of the heading controller is not impaired.

Line of Sight Guidance

The basic guidance law is then given in terms of the Line of Sight Law for use with the autopilot in Eq.(6) is then

$$y(t)_{com(LOS(i))} = tan^{-1}(\tilde{Y}(t)_{wpt(i)} / \tilde{X}(t)_{wpt(i)}) \tag{7}$$

$$\tilde{Y}(t)_{wpt(i)} = (Y_{wpt(i)} - Y(t))$$
$$\tilde{X}(t)_{wpt(i)} = (X_{wpt(i)} - X(t))$$

The position definitions and nomenclature are as given by reference to Figure 2.

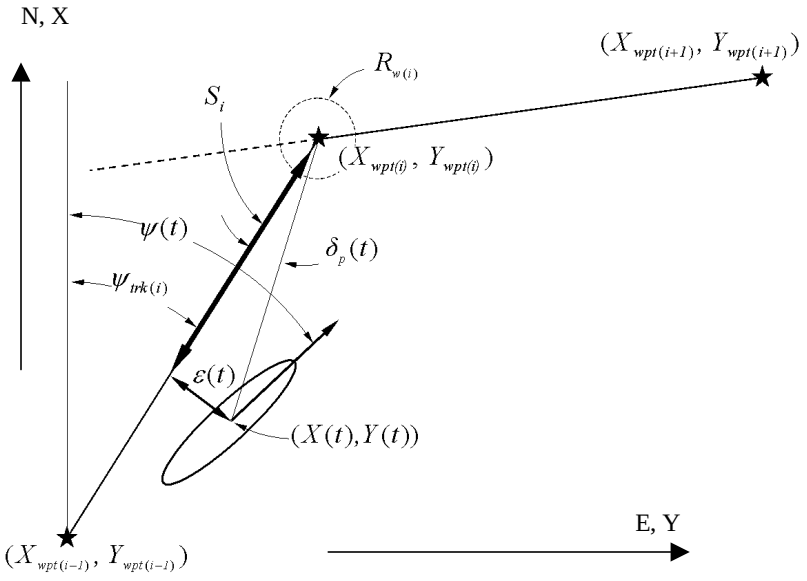

Figure 2. Cross Track Position Error ε(t) Definitions

A typical response for the vehicle track following in the presence of Northerly and Easterly currents of one half a knot is illustrated in Figure 3. In this figure we see that the vehicle heads along the track but is seriously in error with the presence of the cross currents.

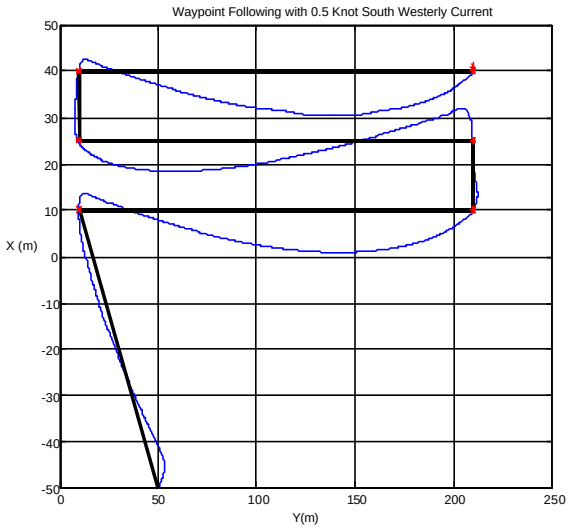

Figure 3, Line of Sight Guidance Only in the Presence of 0.5 Knot Cross Currents

Cross Track Error

The variable of interest to minimize is the cross track error, $e(t)$, and is defined as the perpendicular distance between the center of the vehicle (located at $(X(t),Y(t))$ and the adjacent track line. The total track length between way point i and $i\text{-}1$ is given by

$$L_i = \sqrt{(X_{wpt(i)} - X_{wpt(i-1)})^2 + (Y_{wpt(i)} - Y_{wpt(i-1)})^2}, \quad (8)$$

where the ordered pairs $(X_{wpt(i)}, Y_{wpt(i)})$ and $(Y_{wpt(i-1)}, X_{wpt(i-1)})$ are the current and previous way-points respectively. The track angle, $y_{trk(i)}$, is defined by

$$y_{trk(i)} = tan2^{-1}(Y_{wpt(i)} - Y_{wpt(i-1)}, X_{wpt(i)} - X_{wpt(i-1)}). \quad (9)$$

The cross track heading error $\tilde{y}(t)_{CTE(i)}$ for the i^{th} track segment is defined as

$$\tilde{y}(t)_{CTE(i)} = y(t) - y_{trk(i)} + b(t) \quad (10)$$

where $\tilde{y}(t)_{CTE(i)}$ must be normalized to lie between $\pm 180^0$. $b(t)$ is the angle of side slip and is defined here as

$$tan(b(t)) = v(t)/U$$

When $\tilde{y}(t)_{CTE(i)}$ is nulled, it may be seen that the instantaneous velocity vector then heads along the track with $y(t) = y_{trk(i)} - b(t)$

The difference between the current vehicle position and the next way point is

$$\begin{aligned} \tilde{X}(t)_{wpt(i)} &= X_{wpt(i)} - X(t) \\ \tilde{Y}(t)_{wpt(i)} &= Y_{wpt(i)} - Y(t) \end{aligned} \quad (11)$$

With the above definitions, the distance to the i^{th} way point projected to the track line $S(t)_i$, can be calculated as a percentage of track length using

$$S(t)_i = (\tilde{X}(t)_{wpt(i)}(X_{wpt(i)} - X_{wpt(i-1)}) + \tilde{Y}(t)_{wpt(i)}(Y_{wpt(i)} - Y_{wpt(i-1)}))/L_i \quad (12)$$

The cross track error $e(t)$ may now be defined in terms of the current vehicle position, the previous and next waypoints as

$$e(t) = S_i(t)\tan(d_p(t)) \tag{13}$$

where $d_p(t)$ is the angle between the line of sight to the next way point and the current track line given by

$$\begin{aligned} d_p(t) = {} & \tan 2^{-1}(Y_{wpt(i)} - Y_{wpt(i-1)}, X_{wpt(i)} - X_{wpt(i-1)}) \\ & - \tan 2^{-1}(\tilde{Y}(t)_{wpt(i)} - \tilde{X}(t)_{wpt(i)}) \end{aligned} \tag{14}$$

and must be normalized to lie between $\pm 180^0$.

Line of Sight with Cross Track Error Controller

Cross track error is controlled by the addition of a term in the guidance law proportional to cross track error which provides additional heading to drive to the track path in spite of cross currents. This topic is discussed in detail in Papoulias (1995).

$$y(t)_{com(LOS(i))} = \tan^{-1}(\tilde{Y}(t)_{wpt(i)} / \tilde{X}(t)_{wpt(i)}) - \tan^{-1}(e(t)/r) \tag{15}$$

In the Cross Track Error guidance law above, r is a parameter usually chosen depending on the vehicle turning radius and is commonly between 4-5 vehicle

lengths. Too small a value leads to unstable steering response. It should be pointed out that in dealing with real time control applications with unmanned underwater vehicles, the issues surrounding the wrapping of the heading are troublesome. For control and guidance work we generally bound headings to the sector

$$-180 < y < 180$$

although for filtering work the heading state has to be continuous and wrapped. Figure 4 shows an improved tracking result from this guidance law, even in the presence of cross currents. Steady state errors persist but can be eliminated by an integral of error term if so desired, Figure 5. Notice in Figure 5 that there is an over and undershoot behavior with integral control even though it's magnitude is limited using anti-reset windup techniques.

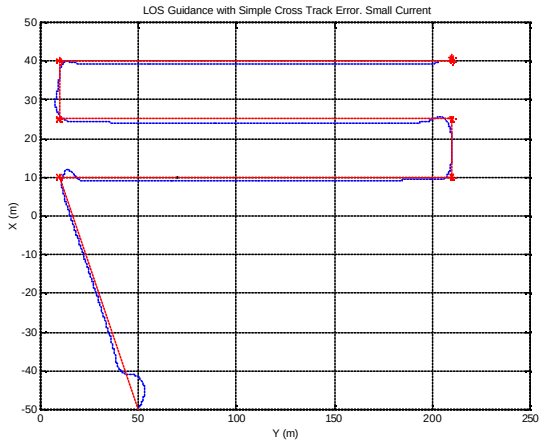

Figure (4) Line of Sight with Simple Cross Track Error Term

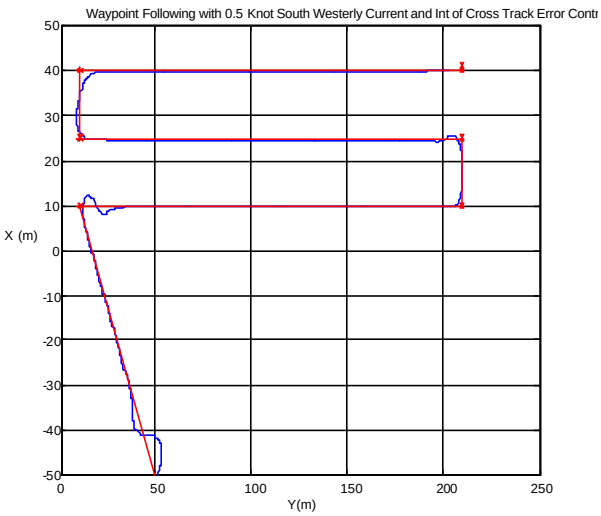

Figure 5 Line of Sight with Cross Track Error Term And Integral Of Error In The Presence Of Cross Currents

One of the problems with this approach is that stability is not guaranteed as part of the design process and depends on the selection of the look ahead distance r.

Sliding Mode Cross Track Error Guidance:

With the cross track error defined, a sliding surface can be cast in terms of derivatives of the errors such that

$$\begin{aligned} e(t) &= e(t) \\ \dot{e}(t) &= U\sin(\tilde{y}(t)_{CTE(i)}) \\ \ddot{e}(t) &= U(r(t)+\dot{b}(t))\cos(\tilde{y}(t)_{CTE(i)}) \\ \dddot{e}(t) &= U(\dot{r}(t)+\ddot{b}(t))\cos(\tilde{y}(t)_{CTE(i)}) - U(r(t)+\dot{b}(t))^2\sin(\tilde{y}(t)_{CTE(i)}) \end{aligned} \tag{16}$$

The question now arises as to how to include the effects of the side slip and its rate of change. We generally make the assumption that the time rate of change of side slip is small compared to the turn rate, *r(t)*, although this depends somewhat on the particular vehicle considered. For the NPS ARIES vehicle, it is typically less than 0.1

rad/sec. and may be neglected. Thus we assume that $\dot{b}(t)$,and $\ddot{b}(t)$ in Equations (16) are negligible.

A sliding surface for the cross track error controller is selected to be a second order polynomial of the form

$$s(t) = \ddot{e}(t) + l_1\dot{e}(t) + l_2 e(t) \tag{17}$$

The reaching condition for reduction of error is

$$\dot{s}(t) = \dddot{e}(t) + l_1\ddot{e}(t) + l_2\dot{e}(t) = -h\tanh(s/f), \tag{18}$$

and to recover the input for control, the heading dynamics Equation (1) are simplified to neglect side slip dynamics reducing to

$$\dot{r}(t) = ar(t) + bd_r(t); \qquad \dot{y}(t) = r(t);$$

and substituting into (18) using (16) we get an expression for $\dot{s}(t)$:

$$U(ar(t) + bd_r)\cos(\tilde{y}(t)_{CTE(i)}) - Ur(t)^2\sin(\tilde{y}(t)_{CTE(i)}) + l_1 Ur(t)\cos(\tilde{y}(t)_{CTE(i)}) + l_2 U\sin(\tilde{y}(t)_{CTE(i)}) \tag{19}$$

Rewriting Equation (17), the sliding surface becomes

$$s(t) = Ur(t)\cos(\tilde{?}(t)_{CTE(i)}) + l_1 U\sin(\tilde{?}(t)_{CTE(i)}) + l_2 e(t). \tag{20}$$

The rudder input can then be expressed using (19) and (18),

$$d_r(t) = \left(\frac{1}{Ub\cos(\tilde{\psi}(t)_{CTE(i)})}\right)\left\{\begin{array}{l} -Uar(t)\cos(\tilde{\psi}(t)_{CTE(i)}) \\ \quad +U(r(t))^2\sin(\tilde{\psi}(t)_{CTE(i)}) - l_1 Ur(t)\cos(\tilde{\psi}(t)_{CTE(i)}) \\ \quad - l_2 U\sin(\tilde{\psi}(t)_{CTE(i)}) - ?\tanh(s(t)/f) \end{array}\right\} \quad (21)$$

where $l_1 = 0.6$, $l_2 = 0.1$, $h = 0.1$, and $f = 0.5$. To avoid division by zero, in the rare case where $\cos(\tilde{\psi}(t)_{CTE}) = 0.0$ (i.e. the vehicle heading is perpendicular to the track line) the rudder command is set to zero since this condition is transient in nature.

Large Heading Error Mode

Heading errors larger than say 40 degrees often occur in operations, especially when transitioning between tracks. It is not uncommon for a 90 degree heading change to be instituted suddenly. Under these conditions, the Sliding Mode Guidance Law breaks down, and a return to the basic Line of Sight Control Law is required. In this situation, the heading command can be determined from

$$y(t)_{com(LOS(i))} = \tan 2^{-1}(\tilde{Y}(t)_{wpt(i)}, \tilde{X}(t)_{wpt(i)}) \quad (22)$$

and the LOS error from

$$\tilde{y}(t)_{LOS(i)} = y(t)_{com(LOS(i))} - y(t), \quad (23)$$

and the control laws used for heading control, Equations (5,6) may be used.

Track Path Transitions:

Based on operational experience, we find it best to seek a combination of conditions in order for the way point index to be incremented. The first and most usual case is if the vehicle has penetrated the way point watch radius $R_{w(i)}$. This is likely if the vehicle is tracking well on its present track with small cross track error. Secondly, most usually at start up, if a large amount of cross track error is present, the next way point will become active if the projected distance to the way point $S(t)_i$ reached some minimum value $S_{min(i)}$, or in simple cross track error guidance, that the projected distance $S(t)_i$ becomes less than the cross track error control distance, r, This is encoded with the transition conditional,

$$if\ \left(\sqrt{(\tilde{X}(t)_{wpt(i)})^2+(\tilde{Y}(t)_{wpt(i)})^2}\le R_{w(i)} \,||\, S(t)_i < S_{\min(i)} \,||\, S(t)_i < r\right) \quad \text{THEN}$$

Activate Next Way Point

OBSTACLE AVOIDANCE

Three forms of obstacle avoidance guidance are considered. Firstly, when an obstacle is detected using the forward looking sonar perception system, some metrology analysis will give size information and if it is determined to be an object to be avoided by steering, a planned path deviation can be used to override the current path requiring the vehicle to follow a deviated path. Criteria are then checked to see if it is safe to return to the original path. Avoidance paths can be evaluated using many

possibilities but circular paths are convenient. Planning and replanning takes place continuously until no further need to avoid is reached when the original path is regained. In the deviation plan, an added heading command is prescribed for the vehicle to follow a circular path until a sufficient deviation from the obstacle is reached at which time, the avoidance plan is ended, returning the vehicle to the original path following behavior.

Planned Avoidance Deviation in Path

In this section a proposed planned path is determined from a circular path that deviates the heading 50 degrees off course over the planning horizon of 20 meters. This is followed by a linear segment until a predetermined cross track deviation is made. This planned approach has the advantage that a predetermined deviation from path is made before the vehicle is released to return to the original path. The amount of deviation from the original path is determined from the characteristics as well as the position of the obstacle as seen by the forward-looking sonar. The generation of the planned deviated path is triggered by the sonar detection of an obstacle coming within the planning horizon (in this case 20 meters) and at a bearing within a planning sector of 45 degrees. The offset of the object from the path is sensed and used in the calculation of the avoidance distance needed.

A predetermined deviation is described using the following pseudocode

```
if (Range(i,1)<20 & abs(Bearing(i,1)) <  pi/4
  & inplan==0),                inplan=1;end;

if (inplan ==1),
      count=count+1;
```

```
        offset=Range(i,1)*sin(Bearing(i,1));

%replace heading command with path planning
command with Radius R=20m, until 50 degrees
deviation is met followed by a straight line
until offset criterion is met;

psi_errorLOS(i)=  psi_comLOS(i) - psi_cont(i)
+ (count)*dt*U/R;
Xdev(i)=R*sin(count*dt*U/20);
Ydev(i)=R*(1-cos(count*dt*U/20));
end;

% limit the heading deviation

if (((count)*dt*U/R) > 50*pi/180) ,
psi_errorLOS(i)=  psi_comLOS(i) - psi_cont(i)
+ 50*pi/180;
Xdev(i)=Xdev(i-1)+dt*U*sin(50*pi/180);
Ydev(i)=Ydev(i-1)++dt*U*sin(50*pi/180);
end;

if (abs(cte(i))>15),
inplan=0;count=0;r_com(i)=0;end;
% back to default plan
```

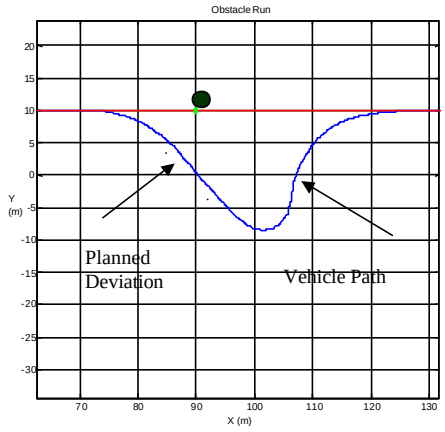

Figure 6 Response of Vehicle to a Planned Deviation in Track

Many different varieties of planned paths are possible. The above is only an example. The point is that using different planning methods, the paths selected are guaranteed to be free of obstacles. Planning for each segment of travel, and considering whether or not to deviate the path can be done continually in sequence every 20 meters or so. If subsequent obstacles are found , deviational paths can be instituted as needed.

Figure 7 below shows the response of the vehicle when a second obstacle is detected while returning to the original track from an initial deviation.

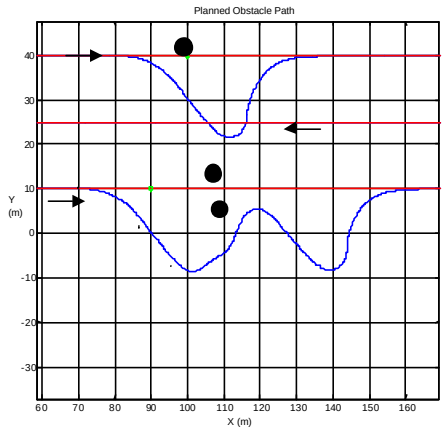

Figure 7 Multiple Obstacles Using the Planned Avoidance Deviation Method

Reactive Avoidance

Reactive avoidance is based on the processing of the forward look sonar image and detection of obstacles from which an avoidance or threat level can be assessed. Based on the threat level the strength of the avoidance action is determined to be either strong or weak. The response is immediate and hence is called reactive.

The model uses a two-dimensional forward-looking sonar with a 120° horizontal scan and a 110-meter radial range. The probability of detection is based on a cookie-cutter approach in which the probability of detection is unity within the scan area and zero anywhere else. Bearing is resolved to the nearest degree and range is resolved every 20 centimeters.

The obstacle avoidance model developed in this work is based on the product of bearing and range weighting functions that form the gain factor for a dynamic

obstacle avoidance behavior. The basis for the weighting functions lies in a fuzzy logic methodology. The weighting functions are MATLAB membership functions from the fuzzy logic toolbox with the parameters selected to maximize obstacle avoidance behavior. The membership function for bearing is a Gaussian curve function of the form:

$$w_1 = e^{\frac{-(x - c)^2}{(2s^2)}} \tag{25}$$

where the parameters *x*, *c*, and *s* are position (or angular position in degrees for the purpose of this model), center, and shape respectively. Shape defines the steepness of the Gaussian curve. The values selected for these parameters to provided sufficient tuning in this membership function were -90:90, 0, 20 respectively. The bearing weighting function can be seen in Figure 8 below.

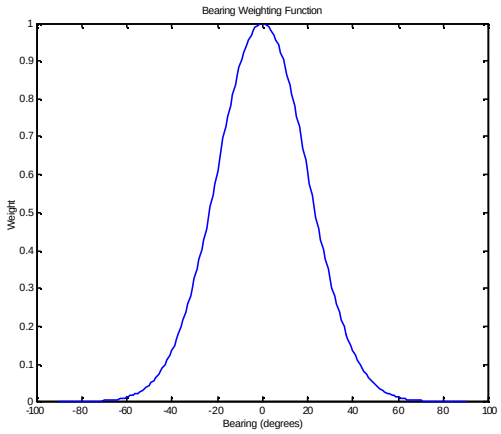

Figure 8. Bearing Weighting Function

The membership function for range is an asymmetrical polynomial spline-based curve called *zmf* and is of the form:

$$w_2 = zmf(x,[a\ b]) \tag{26}$$

where a and b are parameters that locate the extremes of the sloped portions of the curve. These parameters are called breakpoints and define where the curve changes concavity. In order to maximize obstacle avoidance behavior, these values were tuned to be (*sonrange-99*) and (*sonrange-90*). With this selection, the range weight is approximately unity for anything closer than 20 meters and zero for anything farther than 40 meters from REMUS as seen in Figure 9 below.

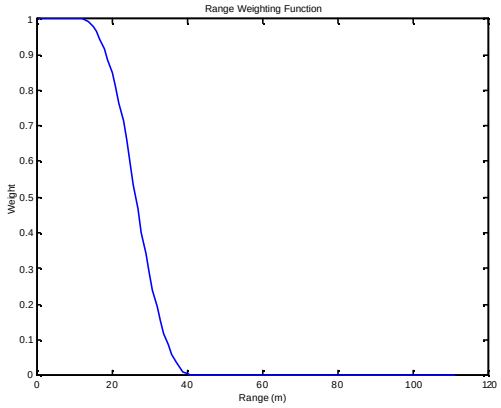

Figure 9. Range Weighting Function,

A final weight based on both bearing and range is calculated from the product of *w1* and *w2*. This weight becomes the gain coefficient that is applied to a maximum avoidance heading for each individual object. The maximum heading is $p/4$ as seen below:

$$y_{oa}(t,c) = w_1 w_2 (p/4) \tag{27}$$

where t is the time step and c is the obstacle being evaluated. The avoidance heading for all obstacles over a single time step (or one look) is then

$$y_{oalook}(t) = \sum_{1}^{c} y_{oa}(t, c) \tag{28}$$

Following an evaluation of each obstacle at every time step, a final obstacle avoidance heading term is determined from the sum of the obstacle avoidance headings of each individual object within a specified bearing and range from the vehicle or

$$y_{oatot}(t) = \frac{y_{oalook}(t)}{cc} \tag{29}$$

where *cc* is the counter used to determine how many obstacles fall into this window. The counter is used to normalize this overall obstacle avoidance term to an average for all of the obstacles within the range above. This bearing and range of the window is determined through a rough evaluation of the weighting functions. In order to fall into the window, the gain factor must be equal to or exceed a value of $w_1 w_2$=0.15.

The obstacle avoidance term $y_{oatot}(t)$ is then incorporated into vehicle heading error as:

$$\begin{aligned} \tilde{y}_{LOS}(t) &= y_{track}(t) - y_{cont}(t) - \ldots \\ &\arctan(e(t)/r) + y_{oatot}(t) \end{aligned} \tag{30}$$

This heading error drives the rudder commands to maneuver around detected objects in the track path.

The initial test performed on the two-dimensional sonar model was navigation around a single point obstacle. This is the simplest obstacle avoidance test for the 2-D

model. Two variations of this test were run for the basic single point obstacle avoidance: a single point on the path and a single point off the path.

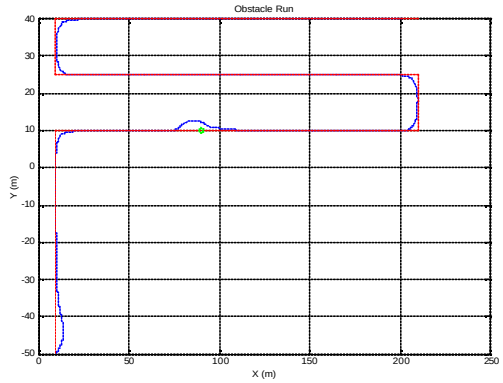

Figure 10a. Single Point Obstacle Run Centerline

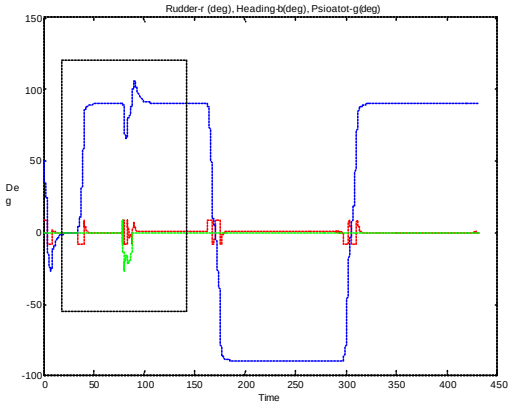

Figure 10b. Single Point Obstacle Run Rudder/Heading/ψ_{oa}

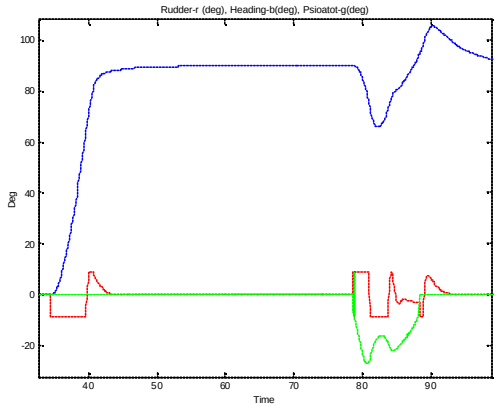

Figure 10c. Zoom of Figure 10b

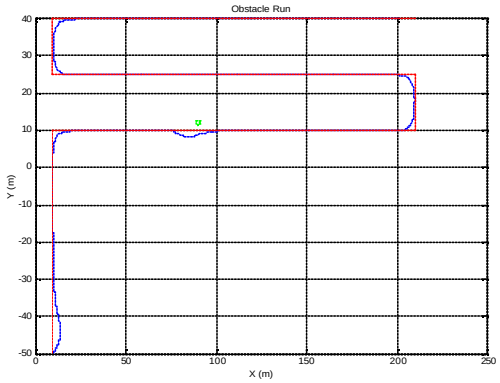

Figure 11 Single Point Obstacle Run Off Path

Figures 10b shows the rudder dynamics, vehicle heading, and obstacle avoidance heading term for the duration of each vehicle run. The rudder action has a direct correlation with the obstacle avoidance heading and overall vehicle heading. The large angle motions of the heading are the ninety-degree turns made to track the ordered vehicle path. There is an associated rudder action with each of these turns as seen by the corresponding rudder curve. These rudder curves show that the maximum programmable rudder deflection is 9°. For all dynamic behaviors, whether associated with a turn or obstacle avoidance maneuver, the rudder initiates the turn with this maximum value. In order to regain track, the rudder action may vary.

A single point obstacle avoidance model is far simpler than a multiple point obstacle avoidance model not only in the maneuvering of the vehicle, but also in maintaining the obstacle picture. For multiple point obstacle avoidance, it is necessary to have a model that reacts to obstacles in a certain proximity to its path rather than all possible obstacles seen by the sonar scan. Weighting functions allow for an accurate compilation of this obstacle picture. The REMUS model builds an obstacle counter for obstacles having a weighting function gain factor ($w_1 w_2$) greater than 0.15. This value allows for a maximum rudder and bearing weight of

approximately 0.386, the square root of 0.15. Referring to the membership functions in Figures 8 and 9, a value of 0.386 correlates to a bearing and range of approximately +/-30° and 30 meters respectively.

As seen in the following figures, REMUS successfully avoids multiple points and multiple point clusters in the same fashion it avoided a single points. The rudder dynamics are minimal during all avoidance maneuvers for an efficient response.

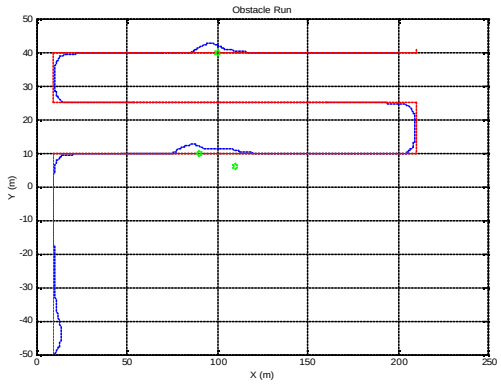

Figure 12 Multiple Point Obstacle Run

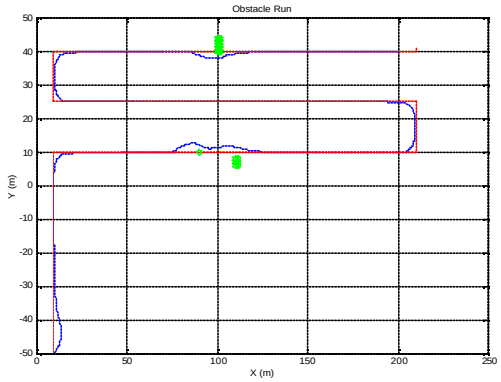

Figure 13 Multiple Cluster Obstacle Run

As seen in Figure 14 below, an obstacle appearing in the vehicle path causes the vehicle heading to deviate from its track path heading of 90° approximately the same amount as the obstacle avoidance heading.

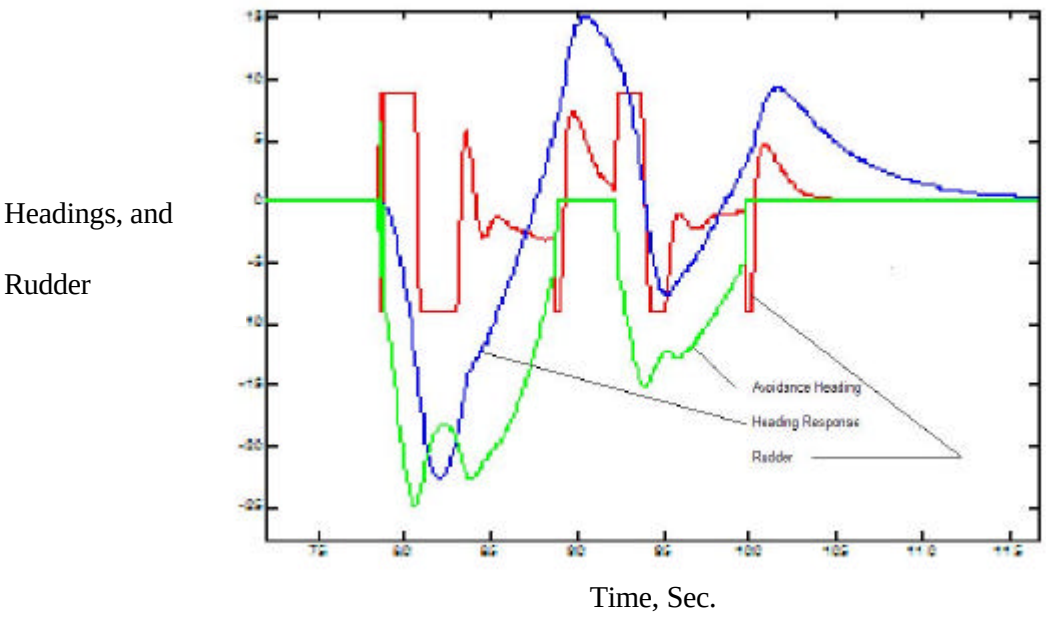

Figure 14. Vehicle Heading Comparison Avoidance Command and Heading Response

ARTIFICIAL POTENTIAL FUNCTIONS

The use of Artificial Potential Functions in Vehicle Guidance is useful in both directing and redirecting vehicle paths as well as in the avoidance of mapped obstacles. Essentially, the local areas in which the vehicle is being guided is mapped into a potential field such that heading commands are derived from the shaping of these potentials. In this manner, obstacles to be avoided are associated with high

potential, free spaces are represented by the valleys and the vehicle guidance seeks minima in the potential field. The motion of the vehicle is taken to be the motion of a particle moving along potential lines. In this work we have considered the use of Gaussian potential functions to provide smooth path following where the paths derived are continuous with continuous derivatives and curvature. This is different from others such as Khatib, 1986, for instance, who used inverse radius potential functions with singularities at the obstacle locations. In all potential function based guidance laws, two potentials must be employed, one to follow the desired path or track and one to avoid any obstacles in the way. While the concepts are quite useful, in some cases instabilities can arise where potential functions combine with vehicle response lags to produce overall instability of path following. It should be intuitive since the potential and hence the guidance heading commands are derived from position based functions. Figure 1 shows the clear role of vehicle position in determining the heading command leading to unstable performance in the guidance loop if commands for reasonable turn rates are not considered carefully. That is, instabilities are possible and smooth paths with curvature limits must be generated. The guidance laws are derived by the following considerations.

Potential Function for Obstacle Avoidance:

Let us define a potential function within the local region Ω in which V has maxima located at the points of obstacles to be avoided: It assumes that a Perception System has detected obstacles and located them so that the locations are known.

$$V(X,Y) > 0 \quad \forall\, (X,Y) \in \Omega \tag{31}$$

If there are obstacles within the region at x_i, y_i, then high potentials are assigned to those points, for example,

$$V(t) = \sum_{i}^{N} V_i \exp[((X(t) - x_i)^2 + (Y(t) - y_i)^2) / 2s_i^2]; \quad (32)$$

A Guidance Law to minimize the potential function is obtained from seeking V to be always reducing along trajectories in (*X*, *Y*). We make

$$\frac{dV}{dt} = V_x' \dot{X} + V_y' \dot{Y} < 0 \quad \forall \; X, Y \in \Omega \quad (33)$$

Leading to

$$\dot{X} = -gV_x' \; ; \; \dot{Y} = -gV_y'; \quad g > 0 \quad (34)$$

and assuming that the vehicle path is commanded to follow tangent paths to the potential lines, a heading command for obstacle avoidance using the artificial potential field can be extracted using

$$y_{oaapf} = \tan^{-1}(V_y' / V_x') \quad (35)$$

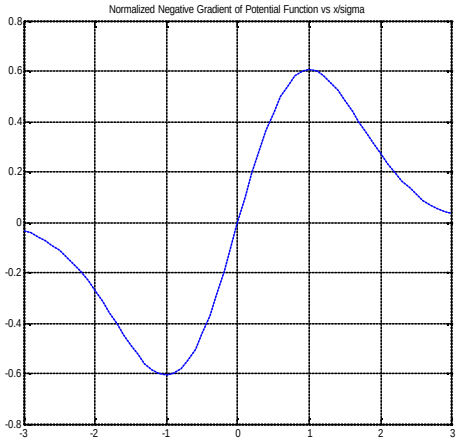

Figure 15 Negative Potential Gradient , $-V_x'$ Vs. Normalized Distance from Center, Sigma = 1.0,

Since *V'* is negative, the avoidance heading steers away from the obstacle. Also in Figure 15 above, it may be seen that the gradient is zero at the origin which does not cause a problem since the origin is an unstable saddle point and paths always steer away from the obstacle.

Multiple Obstacles

With multiple obstacles present, each one has a similar potential that is summed to the total. This gives the more general form for the avoidance command.

$$y_{oaapf}(t) = \tan^{-1} \frac{\sum_{i=1}^{N} (Y(t) - y_i) / s_i^2 * V_i \exp[((X(t) - x_i)^2 + (Y(t) - y_i)^2) / 2s_i^2]}{\sum_{i=1}^{N} (X(t) - x_i) / s_i^2 * V_i \exp[((X(t) - x_i)^2 + (Y(t) - y_i)^2) / 2s_i^2]} \quad (36)$$

An example of three obstacles in the field used in simulation from above is shown in Figure 16.

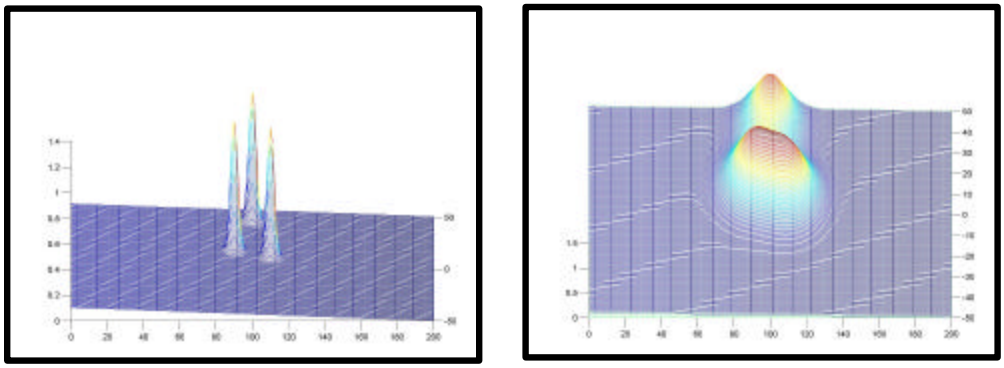

s = 3m. *s* = 10m.

Figure 16, Potential Function Plotted Vertically in the Y vs X Field, *s* = 3 and 10m.

This is not particularly satisfactory alone since the vehicle is already following some defined track and that track has also to be maintained in the absence of obstacles. The problem is solved by the addition of a track following potential $V_{track(i)} = b(1 - S_i)$ in the direction of the current (i) track heading. The total guidance potential becomes the sum of the obstacle avoidance and the track following potentials.

$$V_{track(i)} = \begin{bmatrix} -b_x \\ -b_y \end{bmatrix}; \quad b_x = b\cos(y_{track(i)}); \quad b_y = b\sin(y_{track(i)}) \tag{37}$$

so that the total potential is expressed as $V = V_{track} + V_{oa}$.

This leads to the expression for heading command that includes the track following as well as the obstacle avoidance commands from the potential gradients as in the heading eror for the autopilot $\tilde{y}(t)$

$$\begin{aligned} \tilde{y}(t) &= (y_{track(j)} - y(t)) - \tan^{-1}(e/r) - y_{oaapf}(t) \\ y_{oaapf}(t) &= \tan^{-1}((V'_{oay} + b_y)/(V'_{oax} + b_x)) - y_{track(j)} \end{aligned} \tag{38}$$

The resulting heading controller will judiciously avoid objects while maintaining track. Figure 17 shows the result for three obstacles placed around the planned tracks of the vehicle in which two choices for the parameter b are made.

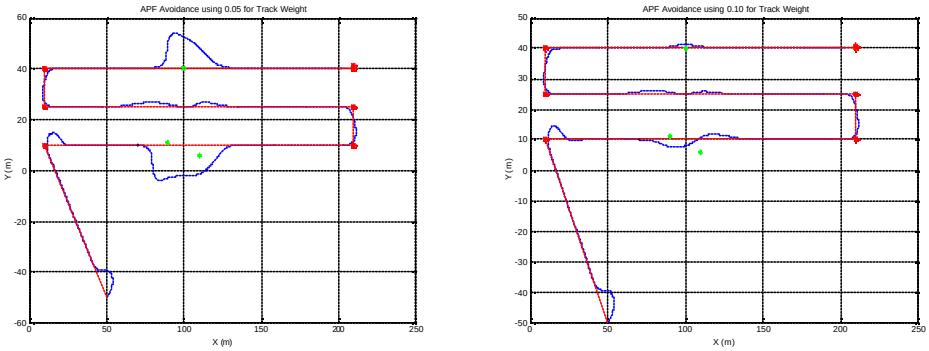

(a), b = 0.05 (b) b = 0.1

Figure 17 Path responses With b =0.05 and 0.1 and σ = 10m.,

Decreasing b in general allows weaker track following when presented with obstacles, increasing b, results in stricter track following and less avoidance. While there are no rules for the selection of b, it would be of interest to relate its choice to the minimum avoidance range. In general, it can be said that b, a gradient, should be scaled according to the selection of the inverse of the standard deviation, s in the Gaussian potentials . Since s_i is a critical distance, it should be chosen with respect to the turning radius of the vehicle. With that said, a choice of b at 0.1 or 0.05 is in order. Where s_i is between 3 and 10 meters. Since the potential gradient is used as the signal for heading change the sharper the gradient the sharper the avoidance turn so that small s_i, leads to sharper turns, and larger s_i lead to softer turns.

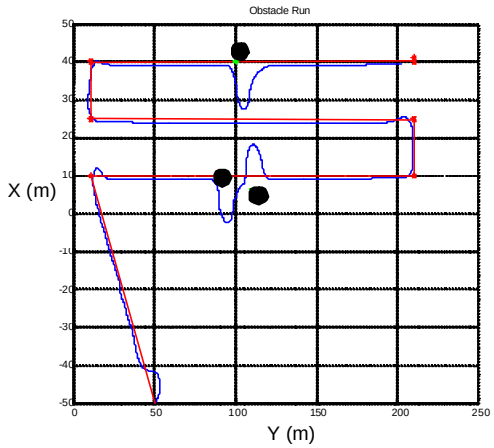

Figure 18 Obstacle Avoidance Gaussian Potential Function with s = 3 m.

Figure 18 shows the avoidance response using b=0.1 and s=3m. in which a responsive deviation is obtained. The minimum avoidance distance for this case is about 4 meters. Varying s produces deviations that increase the initial reaction to avoid with increasing s. However, it is generally found that decreasing s allows more overall path deviation. Thus APFs can be tuned to optimize the path deviation while providing a minimum avoidance radius.

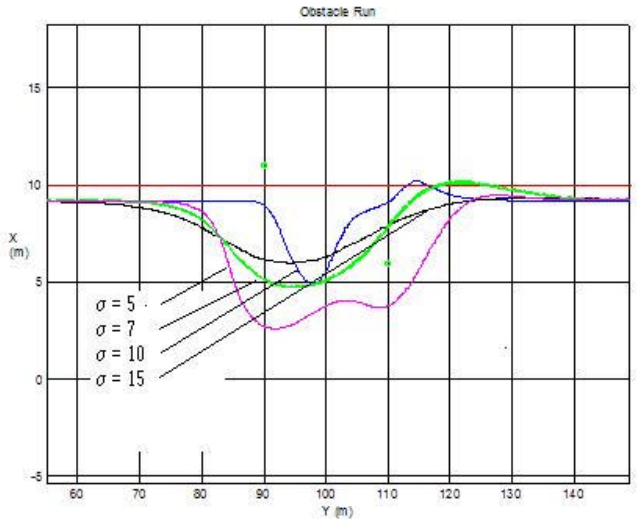

Figure 19. Deviation Paths for s = 5,7,10, and 15m. Showing Smoother Paths with Less Deviation as s Increases

The results of the above simulation have indicated that APFS can be tuned. In the case of Gaussian APFs, the tuning parameters are the standard deviation and the track potential b. These methods can also be embedded into planned avoidance functions since the standard deviations and b values can be selected based on a balancing between path deviation and minimum avoidance distances.

CONCLUSION

In this chapter, guidance laws for track following, cross track error control, and obstacle avoidance using reactive, planned and artificial potential function methods

have been discussed. While more work remains to be done, these methods of avoidance guidance form the basis of most of the needed algorithms. The use of APFs opens up the possibilities of an optimized avoidance plan once obstacles are detected.

ACKNOWLEDGEMENT

The author would like to recognize the input and discussions with Douglas P. Horner especially with respect to the use of APFs, and to Dr. Tom Swean Office of Naval Research for financial support of the work in the Center for AUV Research at NPS.

REFERENCES

Chuang, J. H., "Potential Based Modeling of Three Dimensional Workspace for Obstacle Avoidance", *IEEE Transactions on Robotics and Automation*, v. 14, n. 5, October 1998

Fodrea, L. R., 2001 " Obstacle Avoidance Control for the REMUS Autonomous Underwater Vehicle", MSME Thesis, Naval Postgraduate School, Dec. 2001 http://www.cs.nps.navy.mil/research/auv/theses/fodrea/Lynn_Fodrea/

Fodrea, L. Healey, A. J., "Obstacle Avoidance Considerations for the REMUS Autonomous Underwater Vehicle", *Proceedings of the ASME OMAE Conference*, Paper # OMAE2003-37116, 2003

Healey, A. J., 2001, "Dynamics and Control of Mobile Robot Vehicles", ME4823 Class Notes, Chapters 1-7, http://web.nps.navy.mil/~me/healey/ME4823/

Ge, S. S., Cui, Y. J., "Dynamic Motion Planning for Mobile Robots Using Potential Field Method", *Proceedings of the 8th Mediterranean Conference on Control and Automation (MED 2000)*, Rio, Patras, Greece, 17-19 July, 2000

Kaminer, I. Pascoal, A., Hallberg, E., Silvestre, C., " Trajectory Tracking for Autonomous Vehicles: An Integrated Approach to Guidance and Control", *AIAA Journal of Guidance and Dynamics*, V 21, N 1, pp. 29-38, 1998,

Kanayama, Y., Hartman, B., "Smooth Local Path Planning for Autonomous Vehicle", *International Journal of Robotics Research*, V. 16, N. 3, pp. 263-284, 1997,

Khatib, O., " Real Time Obstacle Avoidance for Manipulators and Mobile Robots", *International Journal of Robotics Research*, v 5, n 1, 1986, pp. 90-98.

Krogh, B. H. and Thorpe, C. E., "Integrated Path Planning and Dynamic Steering Control for Autonomous Vehicles", *Proceedings of the 1986 IEEE International Conference on Robotics and Automation*, Apr, 1986, pp. 1664-1669.

Lane, David M., Petillot, Yvan, and Ruiz, Ioseba Tena, "Underwater Vehicle Obstacle Avoidance and Path Planning Using a Multi-Beam Forward Looking Sonar," *IEEE Journal of Oceanic Engineering*, Vol. 26, n. 1 Apr 2001, pp. 240-251

Latrobe, J. C., “Robot Motion Planning”, Kluwer Academic Publishers, Norwell, MA, 1991.

Marco, D. B., Healey, A. J., 2001, "Command, Control and Navigation: Experimental Results with the NPS ARIES AUV" *IEEE Journal of Oceanic Engineering, Special Issue on Autonomous Ocean Sampling Networks*, vol.26, n.4, Oct.2001, pp.466-477. http://web.nps.navy.mil/~me/healey/papers/IEEE_Marco_Healey.pdf

Milam, M. B., 2003, “Real Time Trajectory Generation for Constrained Dynamics Systems”, Ph. D. Thesis, Caltech, 2003

Papoulias, F. A., “Non-Linear Dynamics and Bifurcations in Autonomous Vehicle Guidance and Control”, *Underwater Robotic Vehicles: Design and Control*, (Ed. J. Yuh), Published by TST Press, Albuquerque, NM. ISBN #0-6927451-6-2, 1995. pp. 41-72.

Prestero, Timothy, 2001, “Verification of a Six-Degree of Freedom Simulation Model for the REMUS Autonomous Underwater Vehicle,” M.S. Thesis Massachusetts Institute of Technology, Sep 2001.

Stentz, Anthony, “Optimal and Efficient Path Planning for Partially-Known Environments”, *Proceedings of the IEEE International Conference on Robotics and Automation (ICRA '94)*, Vol. 4, May, 1994, pp. 3310 - 3317.

Warren, C. W., " Global Path Planning Using Artificial Potential Fields", *Proceedings of the IEEE Conference on Robotics and Automation* pp. 316-321, 1989